EFFECT OF 7% Ni DOPING IN PVP INTERLAYER ON THE FREQUENCY-DEPENDENT ELECTRICAL PROPERTIES OF Au/n-Si SCHOTTKY DIODES UNDER LOW-FREQUENCY CONDITIONS

E.R. BAKHTIYARLI, I.M. AFANDIYEVA

Baku State University, Department of Physics, Baku,Azerbaijan

elvinb18104@sabah.edu.az, I_afandiyeva@yahoo.com

In this study, we investigate the electrical properties of a Au/7%Ni-doped PVP/n-Si metal–polymer–semiconductor (MPS) structure. The study focuses on the influence of the Ni-doped interfacial polymer layer on the device's low-frequency behavior. Electrical characterization was carried out using capacitance–voltage (C–V), conductance over angular frequency–voltage (G/ω–V), and series resistance–voltage (R_s–V) measurements. All measurements were performed at room temperature (300 K), in the voltage range from –4.5 V to +3.5 V, using two low-frequency conditions: 100 Hz and 200 Hz. A pronounced frequency-dependent dispersion was observed in both C–V and G/ω–V characteristics, particularly near +1.2 V, indicating strong interfacial polarization and trap-related effects. The peak capacitance at 100 Hz reached approximately 9.4×10^{-10} F, decreasing at higher frequency due to the reduced response of surface states. Series resistance, extracted using the Nicollian–Brews method, showed significant variation with both voltage and frequency, confirming the active role of interfacial traps and dipolar relaxation in the Ni-doped PVP layer. These findings demonstrate that Ni incorporation substantially modifies the dielectric and resistive properties of the interface, enhancing the sensitivity of the device to frequency-dependent surface state dynamics.

Keywords: Metal–Polymer–Semiconductor (MPS), Ni-doped PVP, Schottky diode, Capacitance–Voltage (C–V), Conductance–Voltage (G/ω–V), impedance spectroscopy, Interface states.
DOI:10.70784/azip.1.2026132

INTRODUCTION

To fully characterize the electrical performance of MPS structures incorporating doped polymer layers, a combination of capacitance–voltage (C–V), conductance–voltage over angular frequency (G/ω–V), and series resistance–voltage (Rs–V) measurements are employed. These techniques are particularly sensitive to interface properties, trap dynamics, and frequency-dependent behavior. The C–V measurement provides insights into the charge distribution, depletion region width, and barrier modification effects induced by the interfacial layer [1-3]. Anomalies such as frequency dispersion, hysteresis, or peak behavior in C–V profiles are strong indicators of interface states or dielectric relaxation phenomena. Conductance measurements, particularly when normalized by frequency (G/ω), allow quantification of the energy loss due to interface trap relaxation. These losses become more significant at low frequencies, where slower processes such as charge exchange with surface states or dipolar reorientation can follow the AC field. Therefore, G/ω–V analysis is indispensable for probing the nature and density of the traps at the metal–polymer–semiconductor interface. Series resistance (Rs) is another important parameter that impacts the real operating conditions of MPS devices [2,4-7]. It reflects not only the resistance of the bulk semiconductor and contacts but also includes resistive contributions from the interfacial layer, especially if it contains trap states, conductive paths, or structural defects. Extraction of Rs from C and G/ω data using models such as the Nicollian–Brews method allows for accurate assessment of the resistive dynamics under forward and reverse bias. Rs tends to vary with frequency and voltage, especially in hybrid structures where interfacial phenomena dominate, and its behavior is critical to interpreting the actual conduction mechanism in the device. Polymers such as polyvinylpyrrolidone (PVP) and polyvinyl alcohol (PVA) are frequently used as interfacial layers and PVP is a linear, water-soluble polymer containing a polar pyrrolidone ring that offers active sites for metal ion coordination [5,7-9]. This ability to host dopants within its structure makes PVP highly adaptable for use in hybrid devices. Similarly, PVA is a polymer rich in hydroxyl functional groups, which not only ensure good adhesion to substrates but also support hydrogen bonding and electrostatic interactions. Both PVP and PVA can be easily processed into uniform thin films through solution-based techniques, allowing precise control over interfacial properties [3,8,10-14]. The doping of polymers like PVP and PVA with metallic elements introduces new electronic states, alters the dipolar character, and enhances the dielectric constant of the material. Transition metals such as Ni, Cu, and Ag are commonly used dopants due to their variable oxidation states and ability to interact strongly with the polymer matrix [2,12,15-18]. In the case of Ni-doped PVP, the metal–ligand interaction between Ni^{2+} ions and the carbonyl oxygen of the pyrrolidone ring leads to the formation of localized electronic states that can influence carrier mobility, trap formation, and dielectric response [19-23]. In light of these considerations, a comprehensive electrical characterization of MPS structures containing Ni-doped PVP as an interfacial layer is essential to understand the combined effects of metal–polymer interaction, trap dynamics, and frequency-dependent dielectric behavior. In the present work, we aim to investigate the Au/7%Ni:PVP/n-Si structure through detailed C–V, G/ω–V, and Rs–V analysis under low-frequency conditions (100 Hz and 200 Hz) at room temperature (300 K), across a voltage range of –4.0 V

131, H.Javid ave, AZ-1073, Baku
Institute of Physics
E-mail: jophphysics@gmail.com

to +3.5 V. The use of low-frequency AC signals allows us to probe the influence of surface states and dipolar relaxation mechanisms, which are more prominent in these conditions due to their slow response times. This study focuses on extracting and understanding the physical processes that occur within the interfacial region, particularly the impact of Ni doping on electrical characteristics, using foundational solid-state techniques that reveal both capacitive and resistive behaviors in detail.

EXPERIMENTAL DETAILS

Fabrication of the Au/7%Ni:PVP/n-Si MPS device began with n-type silicon wafers featuring (100) orientation, approximately 350 μm thickness, and a resistivity range of 1–10 Ω · cm. The wafers were first cleaved and then subjected to a two-step chemical cleaning process: an initial treatment in ammonium peroxide for 1 minute, followed by immersion in a 3:1:1 mixture of H_2SO_4, H_2O_2, and H_2O for 3 minutes. After cleaning, the substrates were thoroughly rinsed using high-purity deionized water (18 MΩ · cm) and dried under a steady nitrogen stream. To establish the ohmic contact, a 150 nm gold layer (99.99% purity) was deposited on the backside of the wafers by thermal evaporation at a vacuum level of $\sim 10^{-6}$ Torr. The samples were then annealed in a nitrogen environment at 550 °C for 5 minutes to enhance contact performance. Formation of the interfacial layer involved applying a 7% Ni-doped PVP solution to the front surface using the electrospinning technique, resulting in a homogeneous and stable film. Once the polymer layer was dried, circular gold contacts with an active area of 7.85×10^{-3} cm² and a thickness of 150 nm were thermally evaporated onto the surface, completing the MPS diode structure. Electrical characterization was carried out by attaching silver-coated copper wires to the electrodes. Throughout the metal deposition process, film thickness was continuously monitored using a quartz crystal thickness sensor integrated into the high-vacuum system.

RESULTS AND DISCUSSIONS

The capacitance–voltage (C–V) and conductance–frequency (G/ω–V), which illustrating in Fig 1, characteristics of the Au/7%Ni:PVP/n-Si structure offer crucial insights into the interfacial electronic properties and the impact of Ni doping within the polymer matrix on the electrical behavior of the hybrid Schottky junction [2-5]. The C–V response at both 100 Hz and 200 Hz demonstrates a characteristic frequency dispersion, with higher capacitance values observed at the lower frequency across nearly the entire voltage range. This behavior can be directly attributed to the enhanced influence of interface states and polarization effects that become more pronounced at low frequencies. At voltages near equilibrium (around 0 V to +1.2 V), a sharp rise and peak in capacitance are evident, suggesting strong charge storage capacity and increased dielectric response due to the presence of mobile or trapped charges at the interface. This peak is more pronounced at 100 Hz, indicating that at lower frequencies, the interface states can effectively follow the AC signal and contribute to the overall capacitance. These interface states, located at or near the PVP/n-Si interface, act as slow traps that can exchange charge with the semiconductor in response to an external electric field. Their dynamic behavior, which manifests as a capacitance increase at low frequencies, diminishes with frequency due to limited response time, leading to the observed dispersion. From a solid-state physics standpoint, Ni ions embedded in the polymer chain are likely to introduce localized states, polarizable centers, and potential hopping sites for charge carriers [19,24]. These centers enhance both space-charge polarization and dipolar reorientation under an AC field, thereby increasing the effective permittivity of the dielectric layer. In turn, this results in elevated capacitance values, particularly in accumulation and near-flatband conditions. The fact that the C–V curves exhibit a smoother increase in the reverse bias region and reach a maximum in forward bias around +1.2 V indicates the transition from depletion to accumulation, with a significant contribution from interfacial polarization mechanisms due to Ni-induced dipole moments and increased trap density. The G/ω–V characteristics further reinforce this interpretation. Conductance increases significantly with applied voltage, peaking near +1.2 V, in correspondence with the capacitance peak. This peak in G/ω, especially more intense at 100 Hz, signifies energy dissipation due to capture and emission of carriers by interface traps. In a typical solid-state dielectric, such peaks indicate relaxation processes—originating either from interfacial dipolar motion or charge hopping between localized states—where the dielectric losses are directly linked to the defect density and dipolar nature of the interfacial layer [13,25-27]. The higher values at 100 Hz compared to 200 Hz confirm that the losses are dominated by slow responding traps, which can efficiently exchange charge at low frequencies but not at higher ones. These traps likely arise from both the natural interface between organic PVP and inorganic silicon, and from the Ni dopant atoms themselves, which disturb the local polymer order and create potential well states that facilitate localized charge capture. Ni doping, at a concentration of 7%, appears to be substantial enough to induce strong dielectric and conductive modulation without completely shorting or metallizing the interface. In fact, the dielectric response is enhanced through localized polarizability while still retaining semiconducting characteristics. The interplay between the Ni-induced dipoles and silicon's native oxide-related traps creates a dense spectrum of energy states capable of interacting with injected carriers

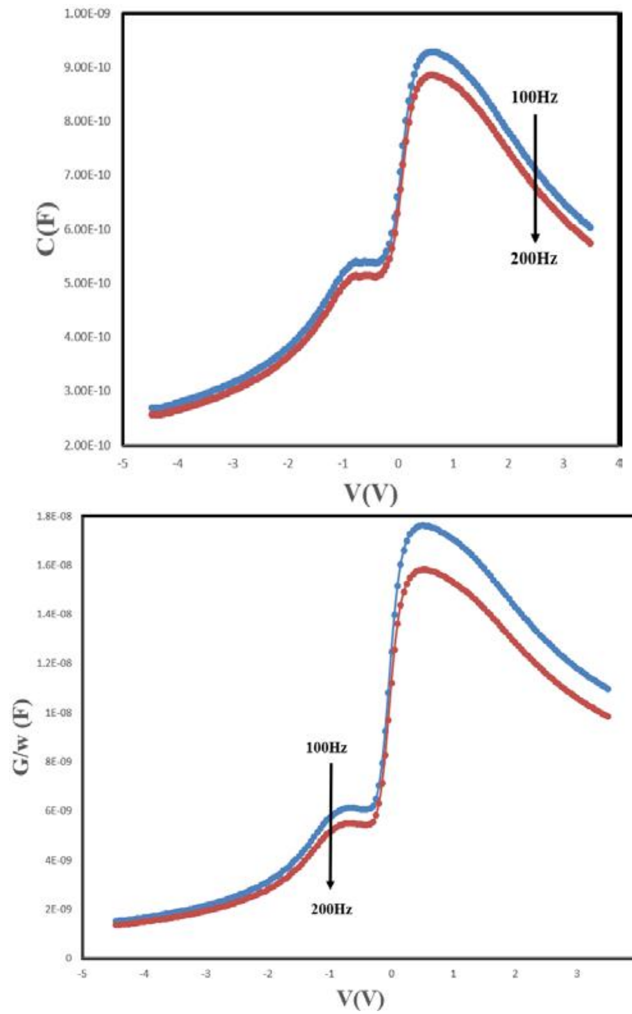

Fig. 1. C-V and G/ω-V plots for 100Hz and 200Hz at -4.5V and +3.5V voltage interval for Au/7%Ni:PVP/n-Si MPS

The R_s–V characteristics of the Au/7%Ni:PVP/n-Si Schottky structure, extracted from the C and G/ω measurements using the Nicollian-Brews method, with following equation and showing in Fig 2, provide essential insight into the resistive behavior of the interface and bulk materials under different bias conditions [1,12-16].

$$R_s = \frac{G_m}{G_m^2+(\omega C_m)^2} \quad (1)$$

The behavior of series resistance as a function of applied voltage is critical to understanding charge transport limitations, interface quality, and the frequency-dependent response of the device. In this structure, the Rs–V curves measured at 100 Hz and 200 Hz display a strong frequency-dependent dispersion and a distinct voltage-dependent profile, revealing the complex interplay between interface traps, carrier mobility, and the resistive properties of the Ni-doped polymer layer. At negative bias voltages, corresponding to reverse bias conditions for the n-type Si, the series resistance is at its highest, exceeding 1 MΩ at 100 Hz and approximately 600 kΩ at 200 Hz. This high resistance region is indicative of a wide depletion layer in the silicon, where the carrier density is low, and the overall conductivity is significantly reduced. In this regime, most of the applied voltage drops across the depletion region, and the current flow is minimal, leading to a high Rs value. As the voltage approaches 0 V, a steep decrease in Rs is observed, more sharply at 100 Hz. This drop corresponds to the flattening of the bands and the onset of forward conduction in the Schottky junction. The reduction in Rs can be linked to the narrowing of the depletion region and the increased availability of free carriers for conduction [27-29,30]. Moreover, this voltage range coincides with the peaks observed in both the C–V and G/ω–V characteristics, suggesting a strong coupling between the resistive and capacitive elements of the junction. At this bias level, interface states and trap centers begin to participate actively in charge exchange, especially at low frequencies, where they can follow the AC signal. The minimum in R_s occurs near the flatband condition, around 0 to +0.5 V, where the depletion region is minimized, and the conduction path is at its most efficient. In this region, the Rs values for both frequencies converge to a lower baseline, indicating that the influence of trap states and dipolar relaxation is reduced, and the conduction becomes dominated by the more intrinsic properties of the device materials. The frequency dispersion observed throughout the Rs–V curve further confirms that charge transport in the Au/7%Ni:PVP/n-Si system is not

purely ohmic but is governed by a combination of resistive and reactive processes. At lower frequencies, traps and dipolar elements have sufficient time to interact with the applied field, leading to increased impedance, while at higher frequencies, these slower processes are bypassed, resulting in a lower effective resistance [19-23,30,31]. This frequency dependence is a hallmark of complex interfacial dynamics and is particularly pronounced in hybrid structures where organic and inorganic materials interact.

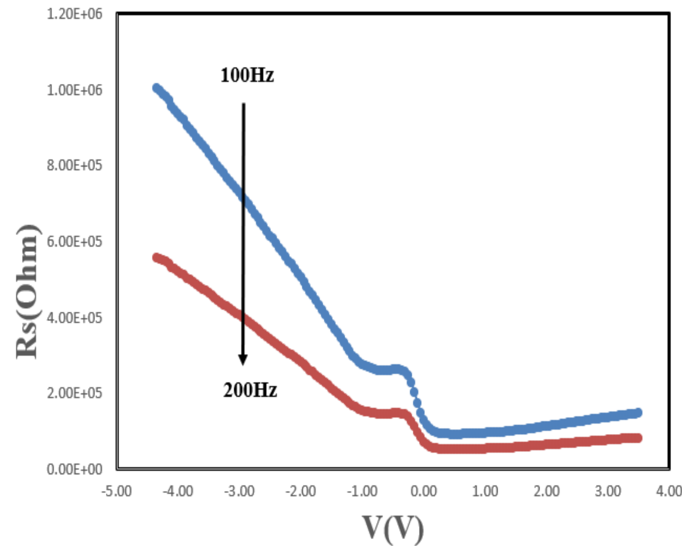

Fig 2. Series Resistance plots for 100Hz and 200Hz at -4.5V and 3.5V voltage interval for Au/7%Ni:PVP/n-Si MPS

The decrease in capacitance and conductivity, as well as the change in R_s and the further increase of this parameter correlate well with the results of [30] and [32]. The obtained result is due to the large contribution of the capacitance of the surface states of C_{ss}. The total capacitance of the contact structure is

$$C = |C_{ss}| + \frac{C_1 C_2}{C_1 + C_2} \quad (2)$$

Where C_{ss} is the capacitance of the surface states, C_1 and C_2 are the capacitances of the space charge region and the dielectric, respectively. An increase in the role of surface states leads to a decrease in the overall capacitance $(\frac{dC}{dV} < 0)$.

CONCLUSION

In this research, the electrical properties of the Au/7%Ni:PVP/n-Si Schottky structure were systematically investigated through capacitance–voltage (C–V), conductance–frequency (G/ω–V), and series resistance–voltage (Rs–V) measurements performed at 100 Hz and 200 Hz. These low-frequency measurements provide detailed insights into interface states, dipolar polarization, and charge transport mechanisms influenced by Ni doping in the PVP layer. The C–V characteristics revealed a pronounced frequency-dependent peak near +1.2 V, with a maximum capacitance of approximately 9.4×10^{-10} F at 100 Hz, decreasing to 8.7×10^{-10} F at 200 Hz. This sharp peak indicates significant interfacial polarization and trap-assisted charge accumulation, particularly pronounced at lower frequencies where interface states can respond more effectively to the AC signal. The frequency dispersion observed in capacitance confirms the dominant contribution of slow interface traps and dipolar orientation mechanisms. The G/ω–V analysis mirrored the C–V behavior, with conductance peaks appearing at the same voltage range. The maximum G/ω value reached $\sim1.7\times10^{-8}$ F at 100 Hz, reducing to $\sim1.55\times10^{-8}$ F at 200 Hz. This behavior highlights energy losses due to charge exchange with interface traps and dipolar relaxation processes, which are more active at lower frequencies. Series resistance values were also strongly voltage- and frequency-dependent. Rs peaked at $\sim1.05\times10^{6}$ Ω at –4 V for 100 Hz and $\sim6.2\times10^{5}$ Ω for 200 Hz, then dropped sharply near 0 V, reaching a minimum of $\sim1.2\times10^{4}$ Ω. The high R_s values under reverse bias confirm reduced carrier mobility and enhanced trap-related resistance. The inclusion of 7% Ni in the PVP matrix significantly increased the interfacial activity, enhancing both dielectric response and trap density. Ni doping introduced dipolar centers and localized states, contributing to higher capacitance, increased dielectric losses, and resistive dispersion—demonstrating its critical role in tailoring the electrical behavior of hybrid organic–inorganic Schottky structures.

[1] *N.A. Al-Ahmadi.* Metal oxide semiconductor-based Schottky diodes: a review of recent advances. Materials Research Express, 7 (2020) 03200; https://doi.org/10.1088/20531591/ab7a60.

[2] *N. Balaram, M. Siva Pratap Reddy, V. Rajagopal Reddy, C. Park.* Effects of high-k zirconium oxide (ZrO_2) interlayer on the electrical and transport properties of Au/n-type InP Schottky diode. *Thin*

Solid Films, 619 (2016) 231–238; https://doi.org/10.1016/j.tsf.2016.10.060.

[3] *S.M. Sze, K.Ng Kwok.* Physics of Semiconductor Devices. (New Jersey: John Wiley & Sons, 2007).

[4] *E.H. Nicollian, J.R. Brews.* MOS (Metal Oxide Semiconductor) Physics and Technology. (New Jersey: John Wiley & Sons, 2002).

[5] *S. Demirezen, Ş. Altındal, Y. Azizian-Kalandaragh, A. M. Akbaş.* A comparison of Au/n-Si Schottky diodes (SDs) with/without a nanographite (NG) interfacial layer by considering interlayer, surface states (Nss) and series resistance (Rs) effects. *Phys. Scr.*, 97 (2022) 055811; https://doi.org/10.1088/1402-4896/ac645f.

[6] *A. Khalkhali, E. Erbilen Tanrıkulu, S. Altındal Yerişkin, A. Arslan Alsaç, K. Yıldız.* A study regarding dielectric response and ac electrical conductivity of Schottky structures (SSs) interlaid with (Fe_3O_4-PVA) by using dielectric spectroscopy method. J. Inorg. Organomet. Polym., (2025); https://doi.org/10.1007/s10904-025-03667-x.

[7] *B. Akın, S. A. Hameed, S. Altındal Yerişkin, M. Ulusoy, H. Durmuş.* The probe of current conduction mechanisms, interface states, and the forward bias intersection point of the Al/Al_2O_3/Ge/p-Si heterostructures depending on temperature. Materials Science in Semiconductor Processing, 184 (2024) 108781; https://doi.org/10.1016/j.mssp.2024.108781.

[8] *İ. Taşçıoğlu, G. Pirgholi-Givi, S. Altındal Yerişkin, Y. Azizian-Kalandaragh.* Examination on the current conduction mechanisms of Au/n-Si diodes with ZnO-PVP and ZnO/Ag_2WO_4-PVP interfacial layers. J. Sol-Gel Sci. Technol., 107 (2023) 536–547; https://doi.org/10.1007/s10971-023-06177-9.

[9] *H.G. Çetinkaya, A. Feizollahi Vahid, N. Basman, S. Demirezen, Y. Şafak Asar, S. Altındal.* On the wide range frequency and voltage dependence of electrical features and density of surface states of the Al/(Cu:DLC)/p-Si/Au Schottky diodes (SDs). J. Mater. Sci.: Mater. Electron., 34 (2023) 822; https://doi.org/10.1007/s10854-023-10247-7.

[10] *A.E. Tezcan, S.A. Hameed, A.F. Vahid, M. Ulusoy, Ş. Altındal.* A study on the complex dielectric (ε*)/electric-modulus (M*)/impedance (Z*), tangent-loss(tanδ), and ac conductivity (σac) of the Al/(S:DLC)/p-Si/Au (MIS)-type Schottky structures in a wide range of frequency and voltage at room temperature (RT). *Physica B: Condensed Matter*, 684 (2024) 415959; https://doi.org/10.1016/j.physb.2024.415959.

[11] *Ç.Ş. Güçlü, M. Ulusoy, Ş. Altındal.* A comparison electrical characteristics of the Au/(pure-PVA)/n-Si and Au/(CdTe doped-PVA)/n-Si (MPS) type Schottky structures using I-V and C-V measurements. J Mater Sci: Mater Electron, 35 (2024) 881; https://doi.org/10.1007/s10854-024-12650-0.

[12] *A.A. Alarabi, O. Çiçek, H. Makara, F. Ünal, M. Zurnacı, Ş. Altındal.* Enhanced sensing capabilities of UV-visible p-n and p-i-n photodiodes using unique layer and contact configurations. Engineering Science and Technology, an International Journal, 62 (2025) 101975; https://doi.org/10.1016/j.jestch.2025.101975.

[13] *A.S. Dinçer, M.T. Haliloğlu, A. Toprak, Ş. Altındal, E. Özbay.* Effect of Si-rich Si_XN_Y multilayer passivation material on the DC electrical characteristics of AlGaN/GaN HEMTs. J Mater Sci: Mater Electron, 34 (2023) 1674; https://doi.org/10.1007/s10854-023-11077-3.

[14] *O. Çiçek, E. Arslan, Ş. Altındal, Y. Badali, E. Özbay*. 21.2 mV/K High-Performance Ni(50 nm)-Au(100 nm)/Ga_2O_3/p-Si Vertical MOS Type Diode and the Temperature Sensing Characteristics With a Novel Drive Mode. IEEE Sensors Journal, 22 (2022) 23699–23704; https://doi.org/10.1109/JSEN.2022.3219553.

[15] *D. Yılmaz, O. Odabaşı, G. Salkım, E. Urfali, B. Çankaya Akoğlu, E. Özbay, Ş. Altındal.* DC and RF performance of lateral AlGaN/GaN FinFET with ultrathin gate dielectric. Semiconductor Science and Technology, 37 (2022) 085008; https://doi.org/10.1088/1361-6641/ac7818.

[16] *A. Chelkowski.* Dielectric Physics. Elsevier, Amsterdam, 1980.

[17] *G. Kandhol, H. Wadhwa, S. Chand, S. Mahendia, S. Kumar.* Study of dielectric relaxation behavior of composites of Poly (vinylalchohol) (PVA) and Reduced graphene oxide (RGO). Vacuum, 160 (2019) 384–393; https://doi.org/10.1016/j.vacuum.2018.11.051.

[18] *M. Sharma, S. K. Tripathi*, Frequency and voltage dependence of admittance characteristics of Al/Al_2O_3/PVA:n-ZnSe Schottky barrier diodes. Materials Science in Semiconductor Processing, 41 (2016) 155–161; https://doi.org/10.1016/j.mssp.2015.07.028.

[19] *O.G. Abdullah, Y.A. Salman, S.A. Saleem.* Electrical conductivity and dielectric characteristics of in situ prepared PVA/HgS nanocomposite films, J Mater Sci: Mater Electron, 27 (2016) 3591–3598; https://doi.org/10.1007/s10854-015-4196-4.

[20] *Y. Badali.* Electrical properties of (PVC:BN) nanocomposite as interfacial layer in metal-semiconductor structure. J Mater Sci: Mater Electron, 35 (2024) 513; https://doi.org/10.1007/s10854-024-12253-9.

[21] *A. Ashery, S. A. Gad, H. Shaban.* Frequency and temperature dependence of dielectric properties and capacitance–voltage in GO/TiO_2/n-Si MOS device, Appl. Phys. *A* 126 (2020); https://doi.org/10.1007/s00339-020-03729-6.

[22] *G.C. Psarras.* Fundamentals of dielectric theories, in: Dielectric Polymer Materials for High-Density Energy Storage, Elsevier, 2018, pp. 11–57; https://doi.org/10.1016/B978-0-12-813215-9.00002-6.

[23] *M. Gökçen, T. Tunç, Ş. Altındal, İ. Uslu.* Electrical and photocurrent characteristics of Au/PVA (Co-doped)/n-Si photoconductive diodes, *Mater. Sci. Eng. B* 177 (2012) 416–420; https://doi.org/10.1016/j.mseb.2012.01.004.

[24] *Ç. Bilkan, Y. Azizian-Kalandaragh, Ş. Altındal, R. Shokrani-Havigh.* Frequency and voltage dependence dielectric properties, ac electrical conductivity and electric modulus profiles in Al/Co_3O_4-PVA/p-Si structures, *Physica B* 500 (2016) 154–160; https://doi.org/10.1016/j.physb.2016.08.001.

[25] *B.K. Jones, J. Santana, and M. McPherson.* Negative capacitance effects in semiconductor diodes, *Solid State Commun.* 107(1988) 47; https://doi.org/10.1016/S0038-1098(98)00162-8.

[26] *S. Bengi, H. G. Çetinkaya, Ş. Altındal, S. Zeyrek.* Examination of Electrical and Dielectric Parameters of Au/n Si Schottky Barrier Diodes (SBDs) with Organic Perylene Interlayer Using Impedance Measurements Under Various Illumination Intensities, *J. Electron. Mater.* 53 (2024) 5606–5616; https://doi.org/10.1007/s11664-024-11213-7.

[27] *S.A. Butcher, T.L. Tansley, D. Alexiev.* An instrumental solution to the phenomenon of negative capacitances in semiconductors, *Solid-State Electronics* 39, 333–336 (1996); https://doi.org/10.1016/0038-1101(95)00143-3.

[28] *X.L. Huang, Y.G. Shin, K.Y. Lim, E.-K. Suh, H.J. Lee, S.C. Shen.* Thermally induced capacitance and electric field domains in $GaAsAl_{0.3}Ga_{0.7}As$ quantum well infrared photodetector, *Solid-State Electronics* 41, 6 (1997); https://doi.org/10.1016/S0038-1101(97)00027-0.

[29] M. Ershov, H. C. Liu, L. Li, M. Buchanan, Z. R. Wasilewski, and A. K. Jonscher, Negative capacitance effect in semiconductor devices, *IEEE Trans. Electron Devices* 45, 10 (1998) 2196–2206; https://doi.org/10.1109/16.725254

[30] *A. Abidinov, I. Afandiyeva, E. Bakhtiyarli, S. Altındal Yerişkin, S.A. Hameed.* Comprehensive Investigation of Negative Capacitance and Inductive Behavior in Pure and 3% and 5% Ni-Doped PVP-Based Au/n-Si (MS) Schottky Diodes (SDs), ACS Applied Electronic Materials 7 (20) (2025) 9399–9407, https://doi.org/10.1021/acsaelm.5c01377

[31] *I.M. Afandiyeva, E.R. Bakhtiyarli, S. Altındal Yerişkin, S.A. Hameed.* Negative dielectric and inductive behavior in Au/n-Si diodes with Ni-doped PVP interlayers, Journal of Materials Science: Materials in Electronics (2026), https://doi.org/10.1007/s10854-026-16574-9

[32] *A.S. Abdinov, I.M. Afandiyeva, E.R. Bakhtiyarli.* Electrical properties and dual barrier phenomena in Au/3% and 5% Ni-doped PVP/n-Si Schottky diodes : role of interlayer engineering, AJP FIZIKA 2025 volume XXXI № 3, section:E, p.23-26.

Received: 16.02.2026